FINAL REPORT OF THE OTKA K 76834 PROJECT
Principal investigator: Dr. Zoltán Csernátony

General
Under the framework of the current project the major goal was to develop, prepare, characterize, formulate and test a new type of biomaterials based on silica aerogels, which were intended for artificial bone substitution.
The materials were designed to provide permeable walls for free oxygen, nutrient and metabolite diffusion/transport to and from the surrounding living tissues, and to be of biodegradable nature, and provide a resorbable solution for bone replacement.

Started from the study of the gelation process of tetraalkoxy silanes, continued through the supercritical drying, testing of additives, developing new formulation and casting techniques, and led to custom-formulated, silica aerogel-based new biomaterials containg hydroxyapatite and tricalcium phosphate particles with or without red flurescence labelling and proven bioactivity both *in vitro* and *in vivo*.

Examination of the gelation process
Chemical compositions (nature of silane reagent) and reaction conditions (base, acid and double catalysis, solvents) were varied as long as an approximately 0,5-1,5 h setting time have been achieved, which proved to be the best for the laboratory casting process. The final process includes tetramethoxy silane (TMOS) as silane reagent, ammonia base catalysis, methanol and water solvent system, and use of gelation retarder additives and guest particles like hydroxyapatite (HA) and tricalcium phosphate (TCP) and results in monolithic pieces.

Effects of additives (filaments, fabrics)
Powder components (HA, TCP, calcium carbonate) were supplied in the process to provide the necessary amount of active phopsphate in the samples, while microcrystalline cellulose was used as a disposable porogen material to provide micron-range pores in the matrix. In order to increase the mechanical stability of the aerogel-based specimens filamental and other type of reinforcements were tested. We have checked the effects of different kind of filaments and fabrics made of glass wool, carbon and Kevlar. It has been proved, that only glass wool and glass facric provided the necessary degree of adhesion, other materials were incompatible with the silica aerogel matrix and resulted in delamination and thread pull-out effects. However, the use of glass wool in the samples intended for animal studies have been sorted out due to the nearly zero resorbsion capability of the laboratory grade glass wool materials.

Properties and biocompatibility of xerogels
Atmospheric ambient drying has also been tested and resulted in significantly shrinked monolithic specimens. SEM and in vitro SBF study indicated that these xerogel samples have the same degree of biocompatibility than the aerogel samples, but their mesoporosity is significanly reduced and the drying process can not be strictly controlled. Mechanical properties of the samples after heat treatment were inferior to aerogel samples due to the high number of microcrackings occured in the ambient drying process.

Reinforcement effects of silica aerogels on PMMA – potential bone cements
Since silica aerogel may behave similarly to Aerosil nanosilica materials, which are widely used in the pharmaceutical industry. We have tested chemically functionalized aerogels as additives in PMMA, which is the base of a large variety of bone cements currently in use. It has been proved that embedding of silica aerogels in PMMA matrix prepared in situ, under

mild conditions significantly enhanced all of the mechanical properties (hardness, impact and compression strength) of their composites and provided significant reinforcing effect. In addition they showed enhanced leaching out under SBF treatment, thus such kind of composites might find applications as bone cement additives in the future.

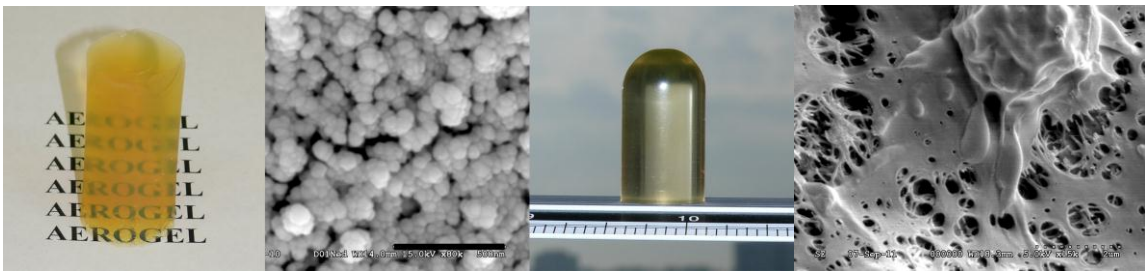

Figure 1 Functionalized aerogel sample, its SEM structure and the monolith recieved after embedding in PMMA. Leaching out of silica from the matrix after SBF treatment, leaving pores behind.

Hydroxyapatite and tricalcium phosphate containing, aerogel-based biomaterials

Silica aerogels containing micron-sized HA and TCP particles were synthesized by the above-mentioned sol-gel technique followed by supercritical drying and heat treatment. Thermal behaviour of the materials has been tested in the 500-1200 °C range and geometry, density and porosity was checked. Organic components and disposable porogenic materials are baked out at 500 °C in several hours with only small changes in dimensions. At higher temperatures shrinking occurs, which turns to be dominant above 900 °C. Exothermic surface reduction start at around 975 °C, simultaneously with the reduction of pore sizes, which leads to the closing of mesopores by 1200 °C. Densities and fracture toughnesses increase with the sintering temperature as expected.

Monolithic pieces were tested for mechanical strength after 1000 °C heat treatment and found that compressive strengths of all specimens exceeded the 8 MPa limit for existing resorbable bone-substitute materials, and in many cases the values were in the 80–100 MPa range, which nearly reaches the compressive strength of the cortical bones. Based on the mechanical properties thus they might be used not just as space-filling materials, but also in load-bearing positions.

Nano-HA has also been tested as quest particle and its composite aerogel provided the highest compressive strength and hardness of all. However, nano-HA proved to be disadvantageous in biocompativity studies and resulted in negligible or no surface HA-layer formation. Consequently, although that material is very strong, can not be recommended for biomedical applications.

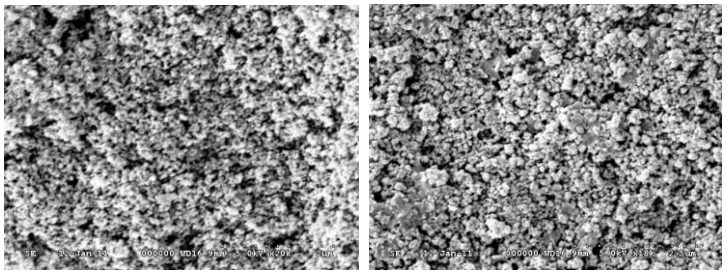

Figure 2 SEM pictures of G5 nano-HA composite sample before and after SBF treatment for 30 days. Virtually no HA layer formation can be observed.

In order to make the composite materials more visible in the live operation theater environment, a new methodology has been developed to prepare europium phosphate labelled tricalcium phosphate particles, which were then embedded in the bone substitute materials. Less than 1% europium content resulted in bright red fluorescence of the samples under 254 nm and less intense fluorescence under 366 nm UV light, and those samples were used in the animal studies. As it is shown in the next figure, red fluorescent granules are well visible under ultraviolet light when they are embedded in bone, or even when are immersed in whole human blood.

For space-filling application a special, granulated formula has been developed by a manual extrusion and cutting technique, which provided at the end of the process cylindrical particles of approx. 1.8 mm diameter. This geometry provides optimal interpaticle space for bone tissue ingrowth.

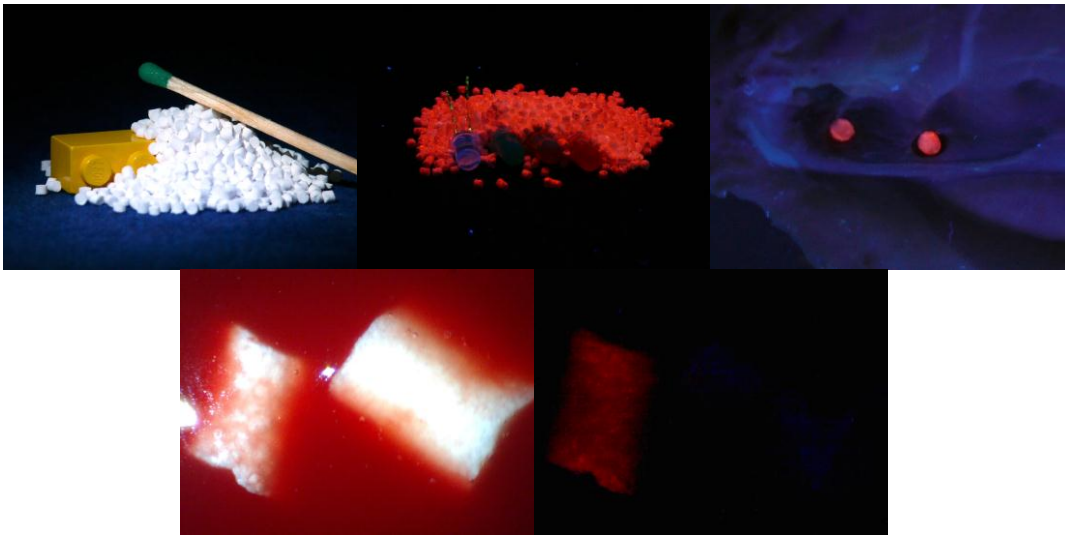

Figure 3 Top row: Granulated red flurescent HA-TCP-silica composite material under visible and UV254 light, and embedded in chicken wing bone tissue. Bottom row: Fluorescent and non-fluorescent particles immersed in whole human blood, under visible (left) and UV254 light (right).

Biocompatibility of the granulated HA-TCP-silica composite materials were checked by immersion in traditional SBF solution. All samples proved to be active in 10 days and showed significant HA layer formation on their surfaces as shown by SEM and EDX elemental analysis results.

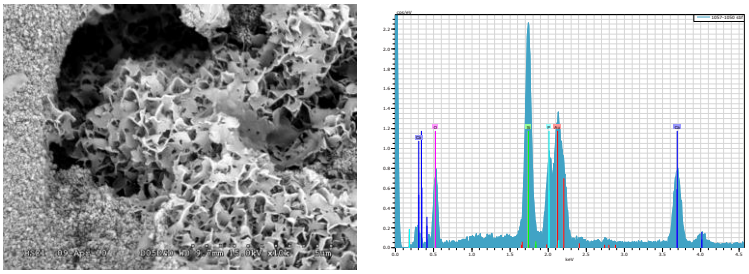

Figure 4 HA layer formation on the surface of a granule of red fluorescent HA-TCP-silica composite, and EDX spectrum of the layer showing strong calcium and phosphorus peaks.

For animal studies (in the future) larger blocks of the composite materials were prepared. In order to provide the necessary macrochannels for bone tissue ingrowth, both disposable and reusable templates were applied and 2D cgannels and 3D frameworks were created. The sizes of the templates were calculated by using the data derived from the heat treatment studies and all were in the 0.8–1.6 mm range. Such kind of channels shrinked to the required 300-400 micron diameter on high temperature heating.

Surgical application generally require irregular shapes of artificial bone substitute materials. To provide the possibility of direct transferring CAT data to computerized work stations, a suspended sintering technique was developed. The material is heated at 1000 °C for one hour to recieve a machinable specimen, which can be drilled and machined afterwards. The final strength, size and hardness can be set by a final heat treatment at 1050 °C.

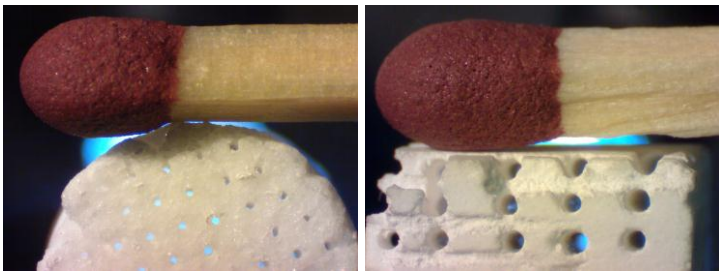

Figure 5 Formation of 200-400 micron diameter 2D and 3D channels were achieved either by reusable or disposable samples.

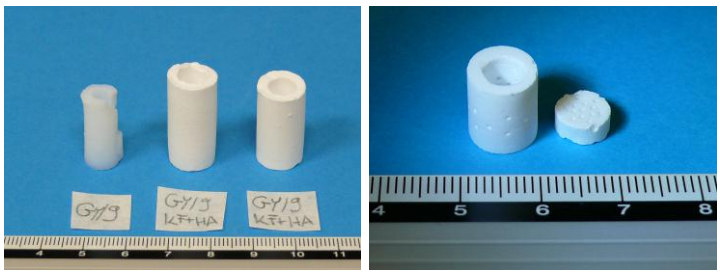

Figure 6 Mold-casting technique of HA-TCP-silica composite resulted in tubular specimens, which were machined after a 1000 °C sintering. A second heat treatment at 1050 °C gives of high mechanical strength hard materials, which hold 300 micron channels in designed arrangement and orientation.

Development of a new simulated body fluid

Standard in vitro biocompatibility test of artificial bone substitute materials is soaking the specimens in simulated body fluids, which composition is similar to the inorganic composition of blood serum. Formation of surface hydroxyapatite layer is considered a sign of biocompatibility and bone formation potential. Standard SBF has the disadvantage of beeing free of ordinary organic components present in the human blood, like amino acids and proteins. It has been shown that proteins may modify the HA-formation potential. We have developed two new simulated body fluids, which contain amino acids at the same concentration, which is present free in the human blood (see Table). Biocompatibilities of our samples were tested simultaneously in traditional ad new SBFs. It has been stated that no difference can be observed in the surface HA layers, thus the compositions can be used as test solutions. It has also been observed that, maybe due to the presence of amino acids, the test solutions are prone to bacterial infection, thus sterile filtration of the solutions and sterilization of the samples are required.

Table 1 Ionic compositions of traditional and newly developed simulated body fluids. Further components are the following amino acids at the given concentrations: glutamine, alanine, glycine, proline, leucine, lizine, serine, valine at 0,52 mmol/L, 0,37 mmol/L, 0,24 mmol/L, 0,21 mmol/L, 0,12 mmol/L, 0,18 mmol/L, 0,12 mmol/L, 0,23 mmol/L, respectively.

Ionic compositions of simulated body fluids					
Ion	**Human plasma (mmol/L)**	**SBF Kokubo (mmol/L)**	**Experimental SBF (mmol/L)**		
			Traditional (SBF)*	**Amino acid High bicarbonate**	**Amino acid Low bicarbonate**
Ca^{2+}	2.5	2.5	2.51	2.51	2.51
HPO_4^{2-}	1	1	1.02	1.02	1.02
Na^{+}	142	142	142	142	142
Cl^{-}	103	148.5	148.0	103	103
Mg^{2+}	1.50	1.50	1.50	1.50	1.50
K^{+}	5.00	5.00	5.07	5.07	5.07
SO_4^{2-}	0.5	0.5	0.52	0.52	0.52
HCO_3^{-}/CO_3^{2-}	27.0	4.2	4.27	27.0	4.20
TRIS buffer			5.00	5.00	5.00

* from ref.: Material and Design 30 (2009) 3920-3924

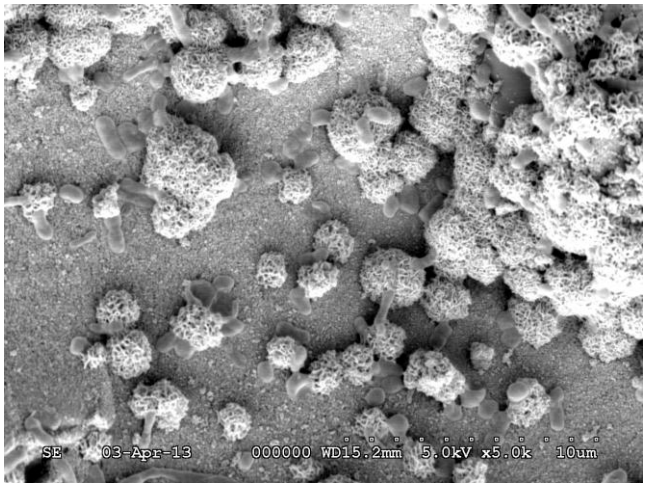

Figure 7 Formation of HA globules in High Bicarbonate Amino Acid SBF solution after 10 days soaking can be observed on the surface of a HA-TCP-silica composite bone substitute sample by SEM. Rod-like formations are identified as common bacteria attached to the surface, indicating that the new SBF solution provides a viable environment.

Application of aerogel matrices in microfluidic chips

Unique properties of functionalized silica aerogels provided the possibility to be used as stationary phase in microfluidic chip for the separation of organic dyes. It has been found that the high porosity and specific surface area and the low flow resistance of the aerogel filler resulted in very rapid baseline separation of two dyes in 18 s time, and can be considered as a new generation of stationary phases for disposable microanalytical devices.

Animal experimentations

The animal experimentations were performed on the left thigh bone of male adult Long-Evans rats, the average weight being 400 g. The anaesthesized rat’s left thigh bone was exposed after

shaving, skin disinfection, and draping. A longitudinal incision was used at the part of the left thigh bone closer to the knee joint, the muscles were split inline with the incision. A 2 mm drill hole was made on the thigh bone, and filled with one of the four materials being tested, or a bone substituting material already available, and in one case it was left empty to be used as a control.

Altogether 65 animals were operated on, of which 8 died either before the operation (aneasthesiology complications) or immediately after (aspiration). Of the remaining 57 animals 6 was not suitable for histological study due to deep infection. 51 samples were sent for histological examination of which 16,12,10, and 8 contained the material being examined respectively, 4 contained the bone substituting material already available, and 1 was used as a control.
Radiological examination of the thigh bone was performed at 4-8-12 weeks after the operation to determine the absorption of the tested material.

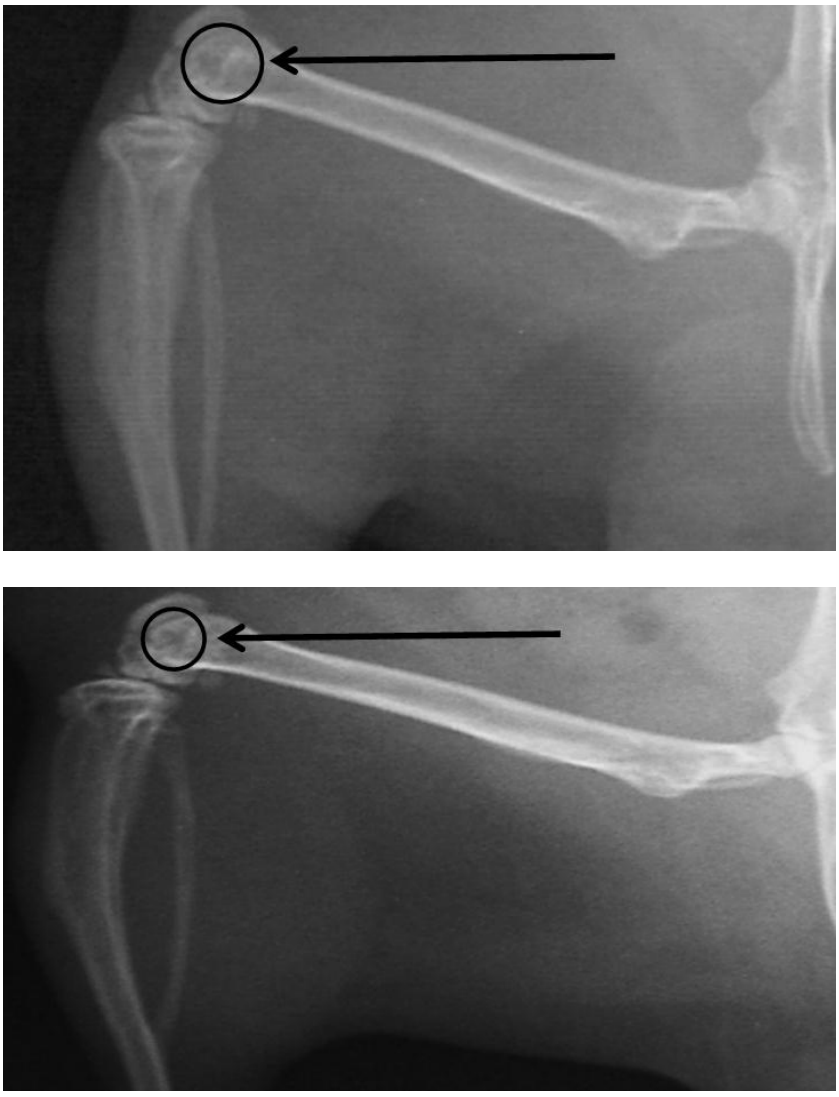

Figure 8 X-rays from the implanted material at 4 and 12 weeks after the operation.

Histological examination showed promising results of bone formation near the tested material. Bone healing and absorption of the bone substitute could be seen on the slides.

The most promising result was shown by material number 1134. In order to examine the dynamics of bone formation caused by the tested material additional animal experimentations were needed. For the additional animal experimentations 16 male Long-Evans rats were operated on, of which 8 was used as a control group and 8 was filled with material number 1134 according to the previously mention surgical technique.

After the removal of the entire femur histological preparation were made from the area under examination. The preparations were stained with Heamotoxilin-Eosin and Van Gieson, and were examined at 2.5x, 5x and 15x magnification with a polarized light microscope at 4, 6, 8 and 12 weeks after the surgical intervention.

4 weeks after the surgical intervention
control (2.5x):

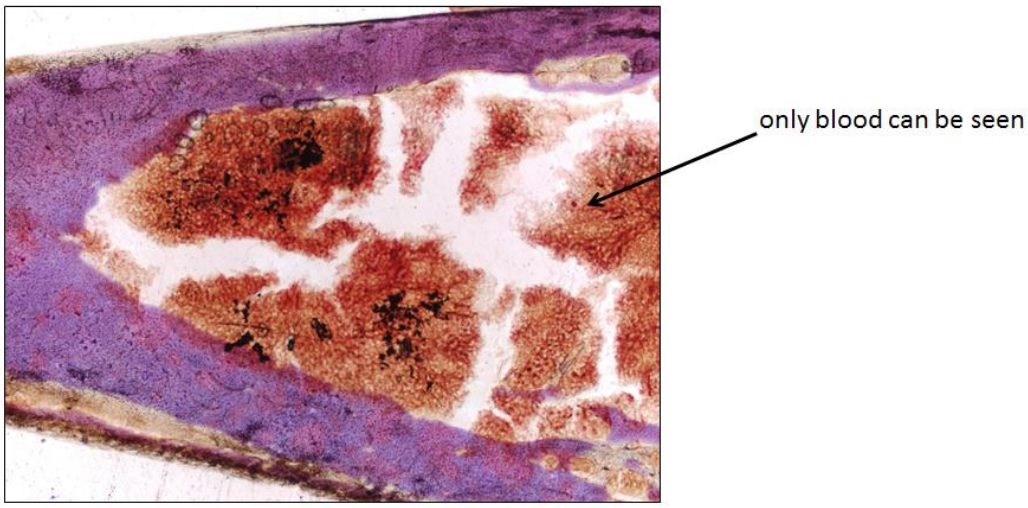

control in polarized light (2.5x):

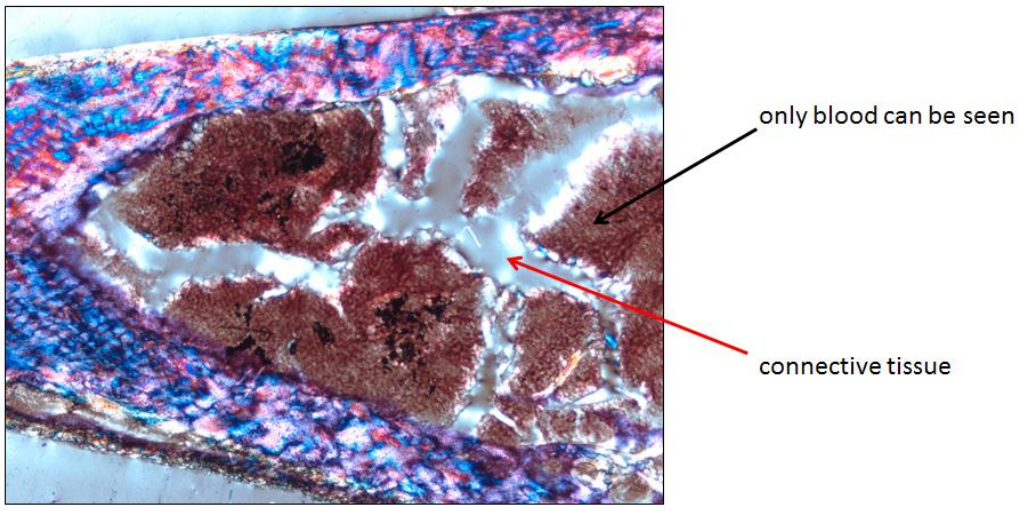

the implanted material (2.5x):

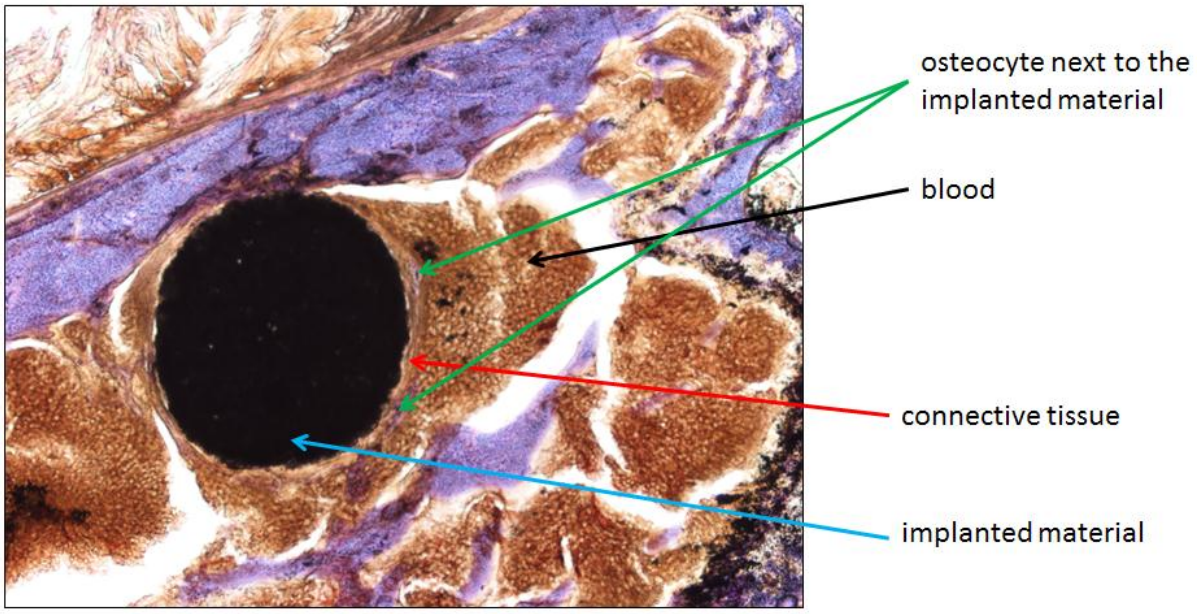

the implanted material in polarized light (2.5x):

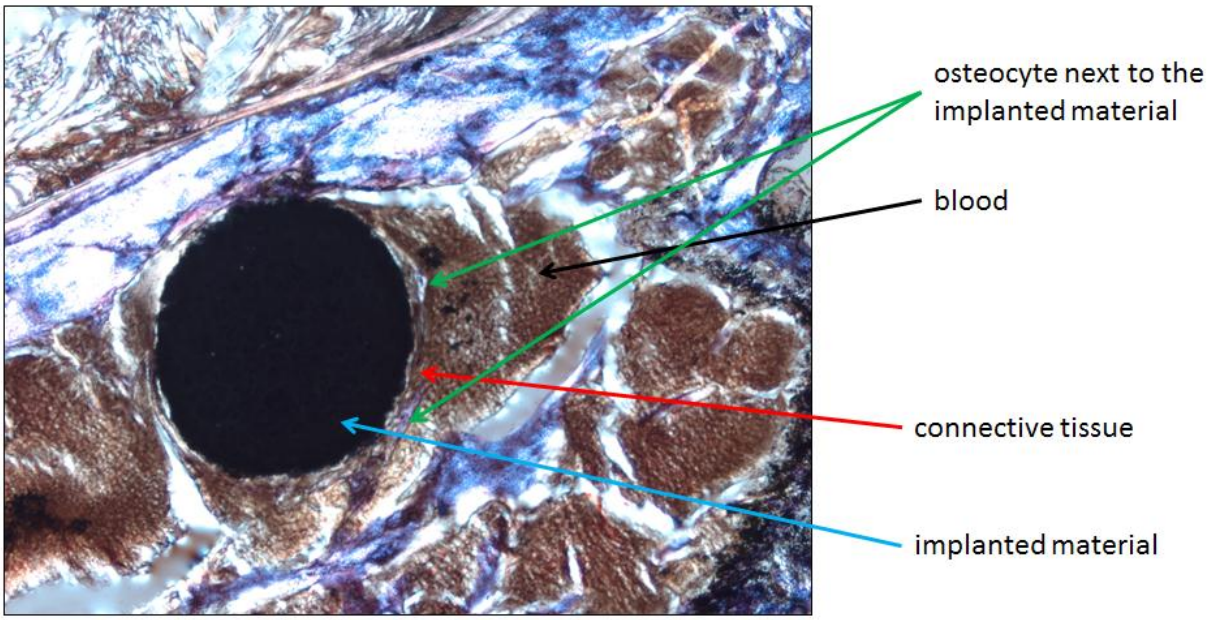

6 weeks after the surgical intervention

control (2.5x):

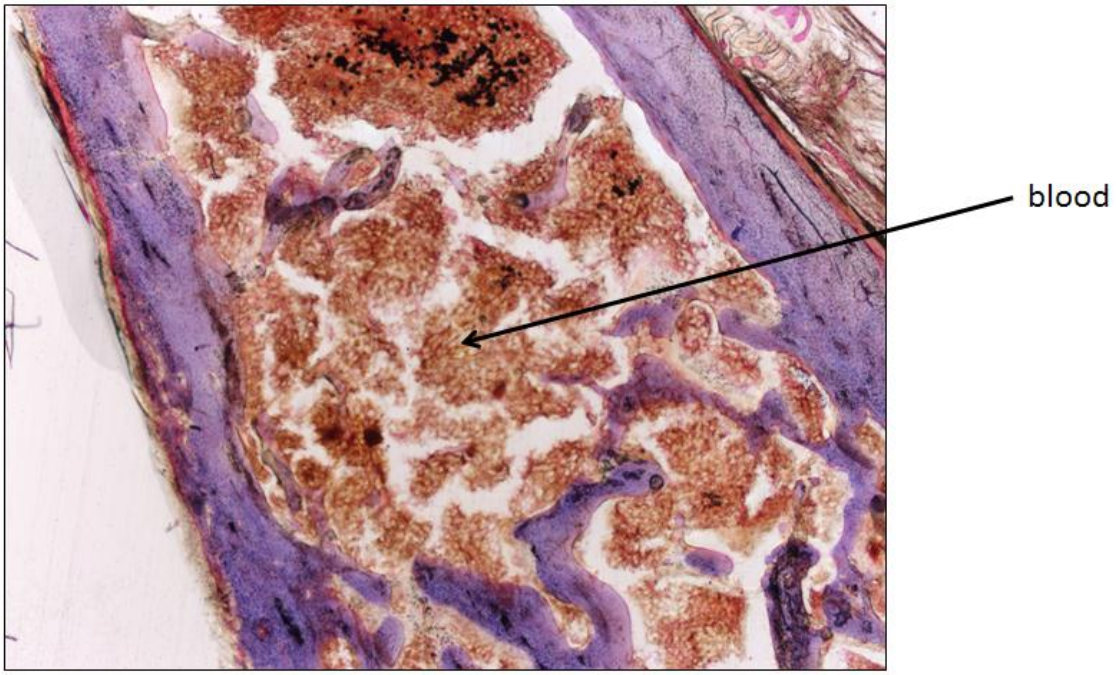

control in polarized light (2.5x):

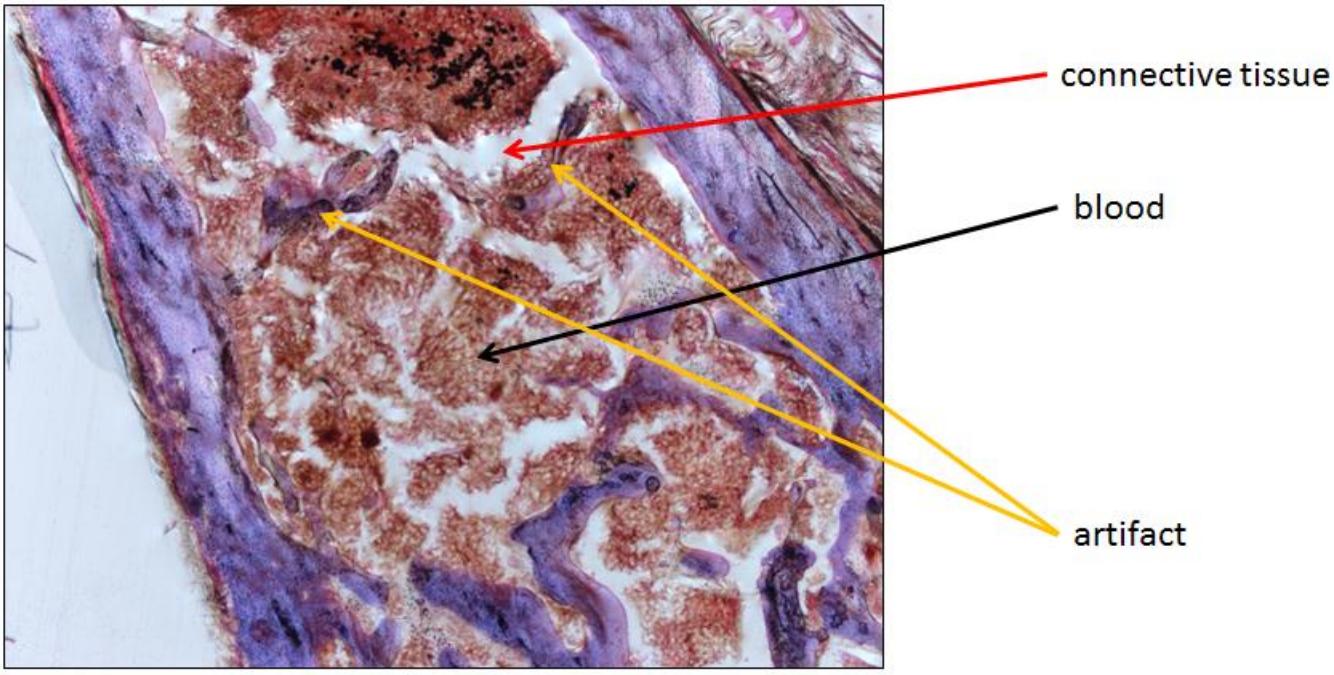

the implanted material (2.5x):

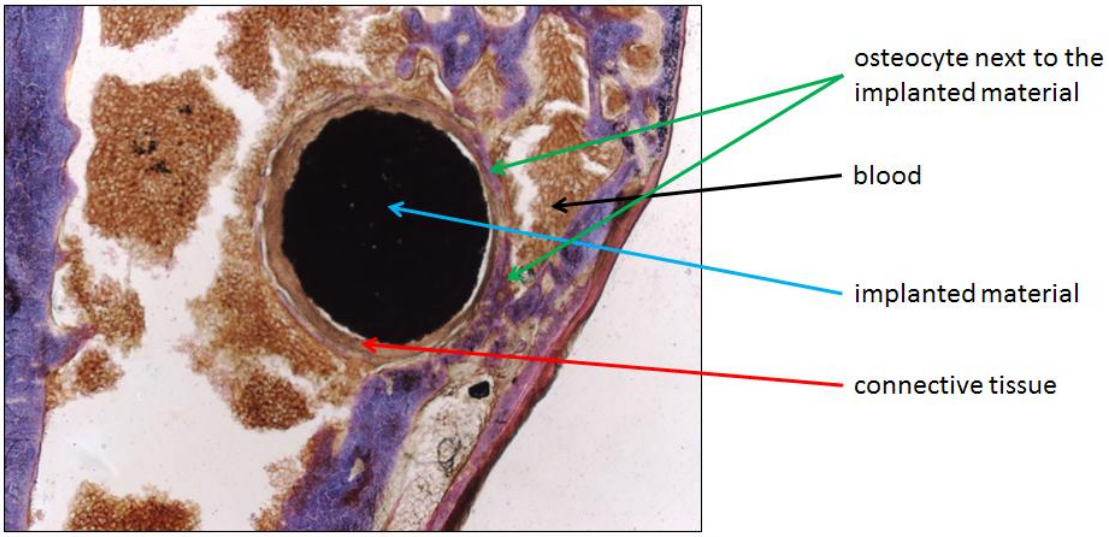

the implanted material in polarized light (2.5x):

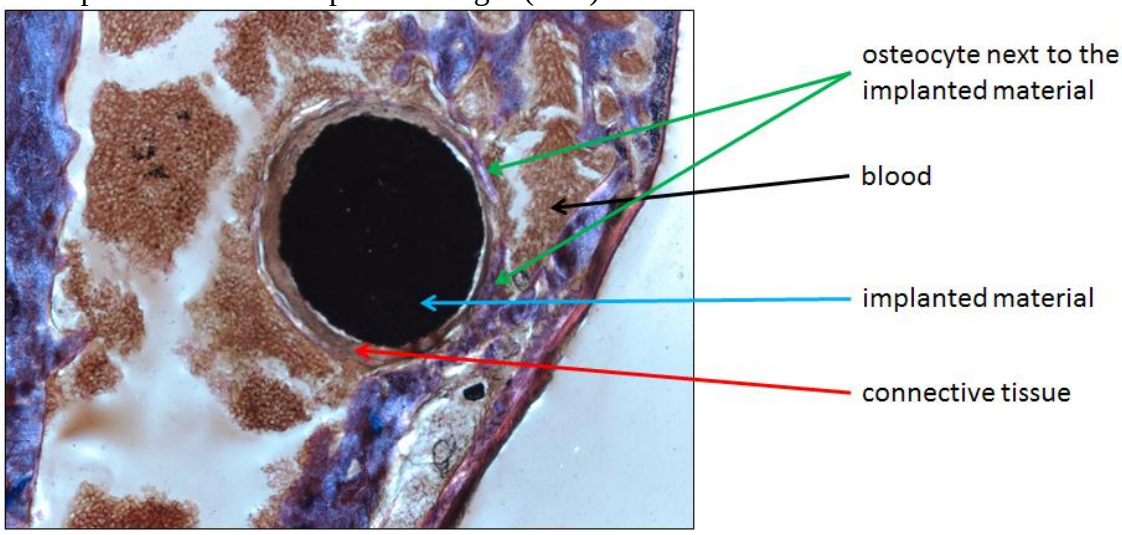

the implanted material (van Gieson, 2.5x):

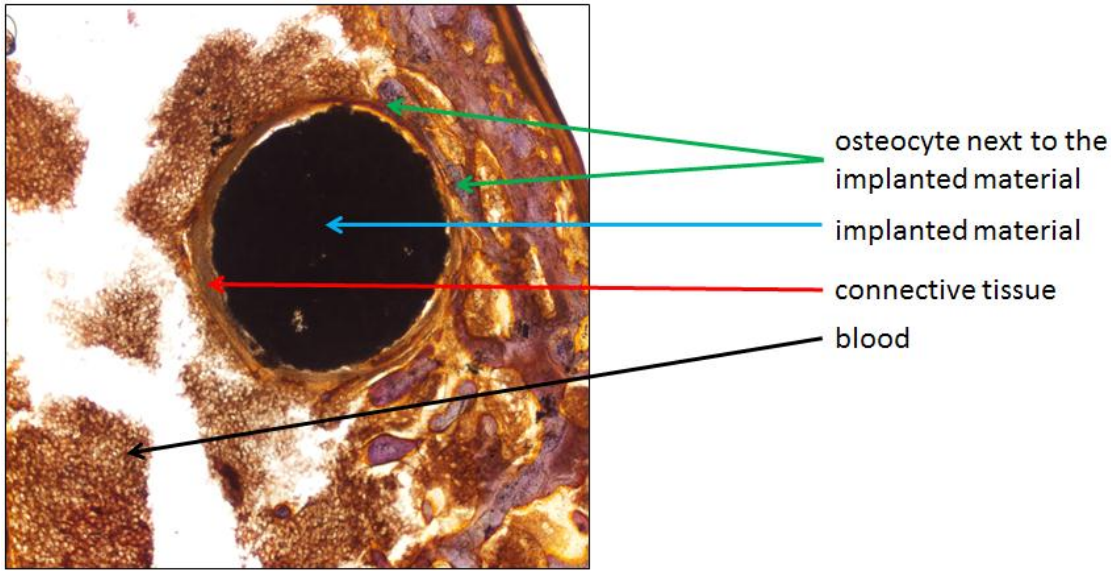

8 weeks after the surgical intervention

control (2.5x):

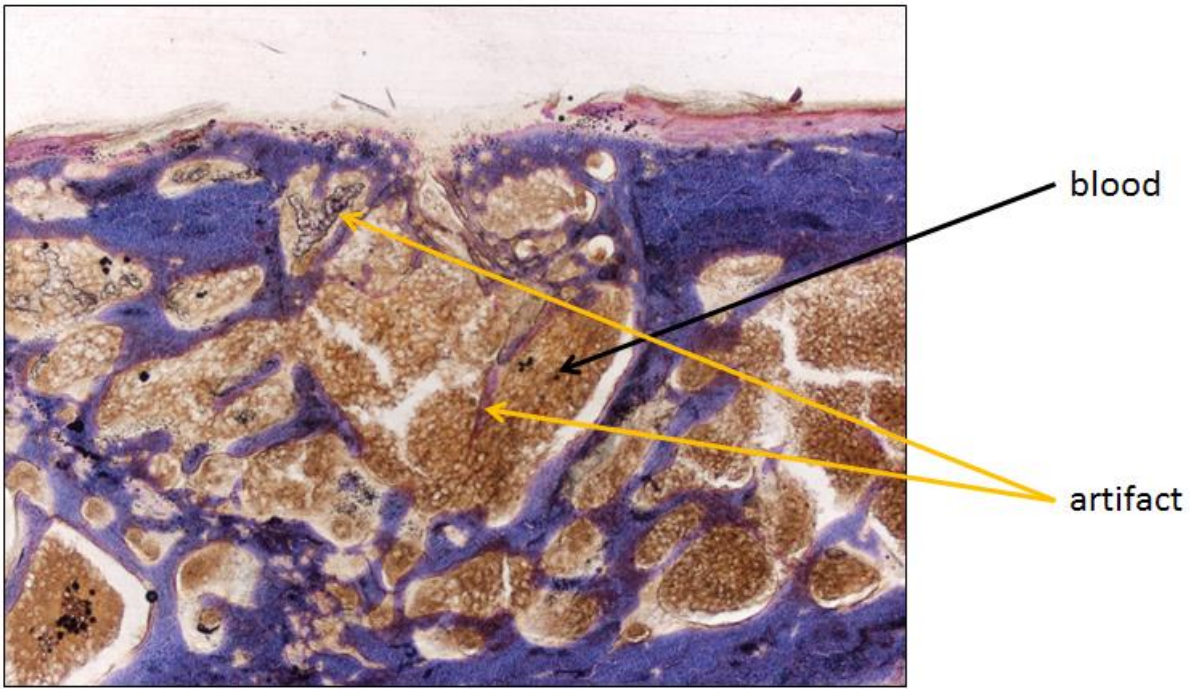

control in polarized light (2.5x):

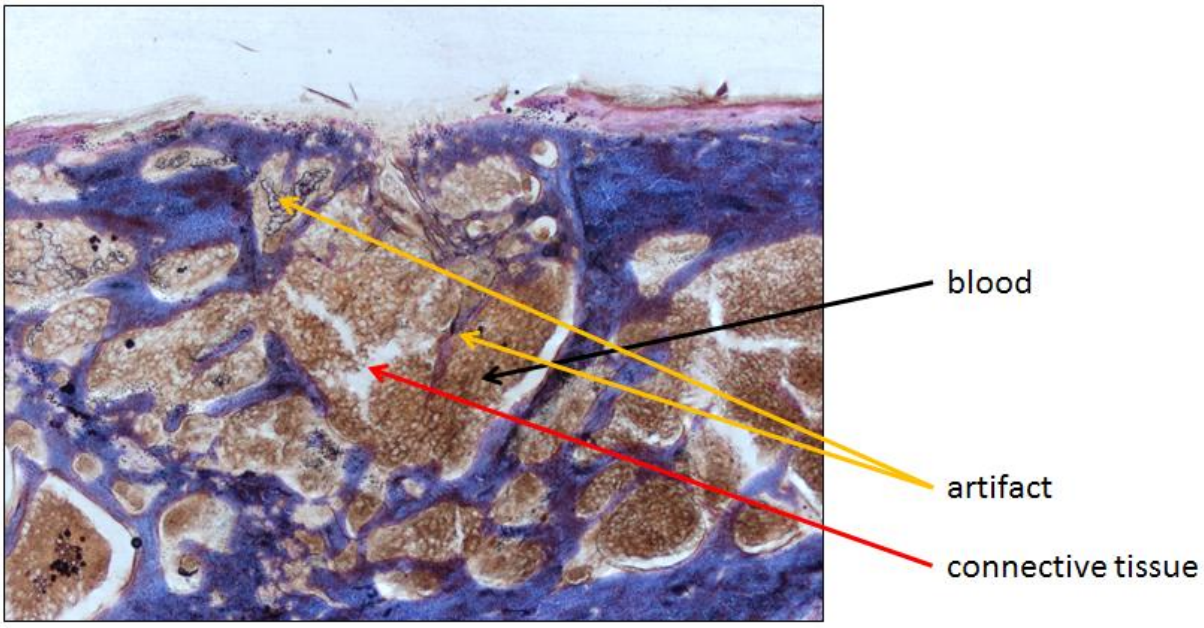

the implanted material (2.5x):

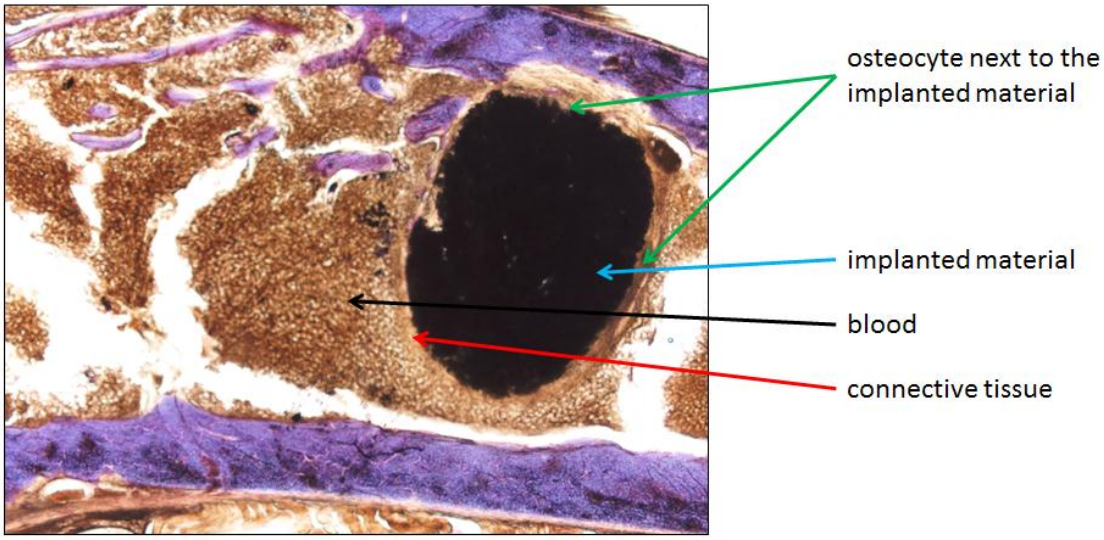

the implanted material in polarized light (2.5x):

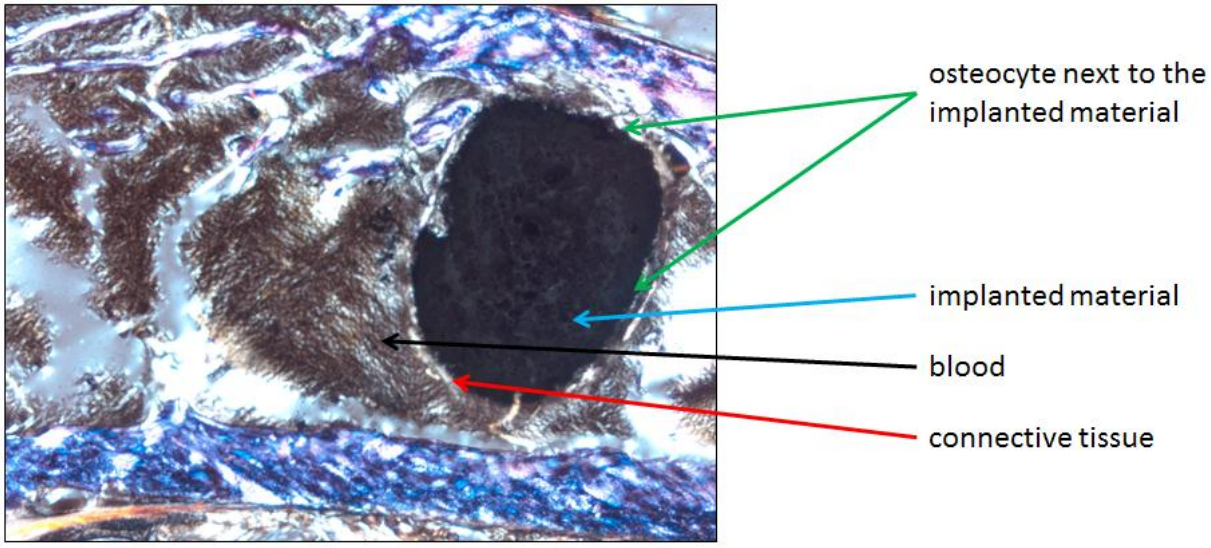

the implanted material in polarized light (5x):

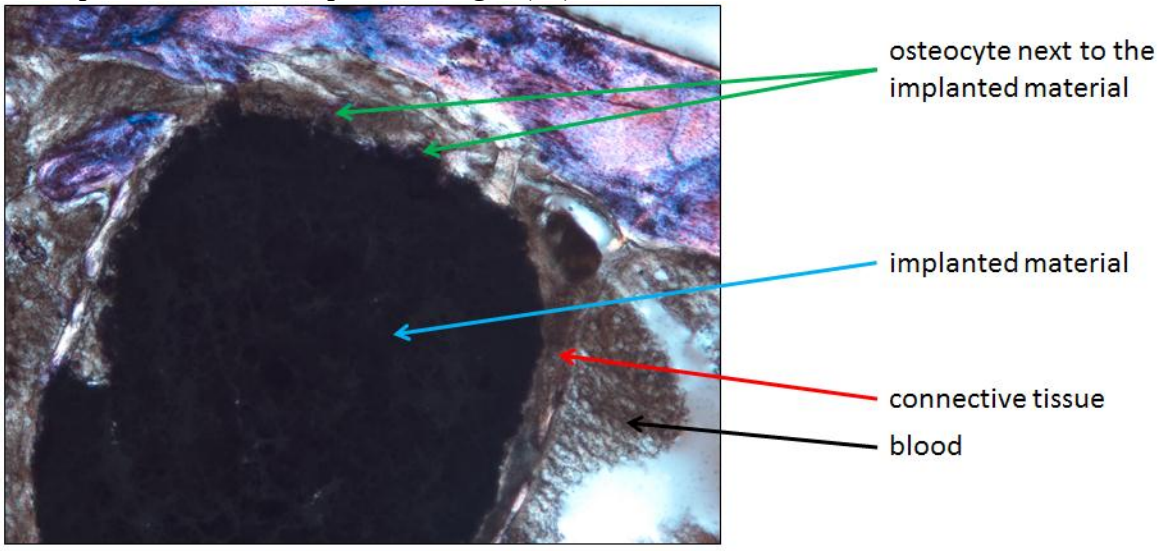

the implanted material in polarized light (van Gieson, 2.5x):

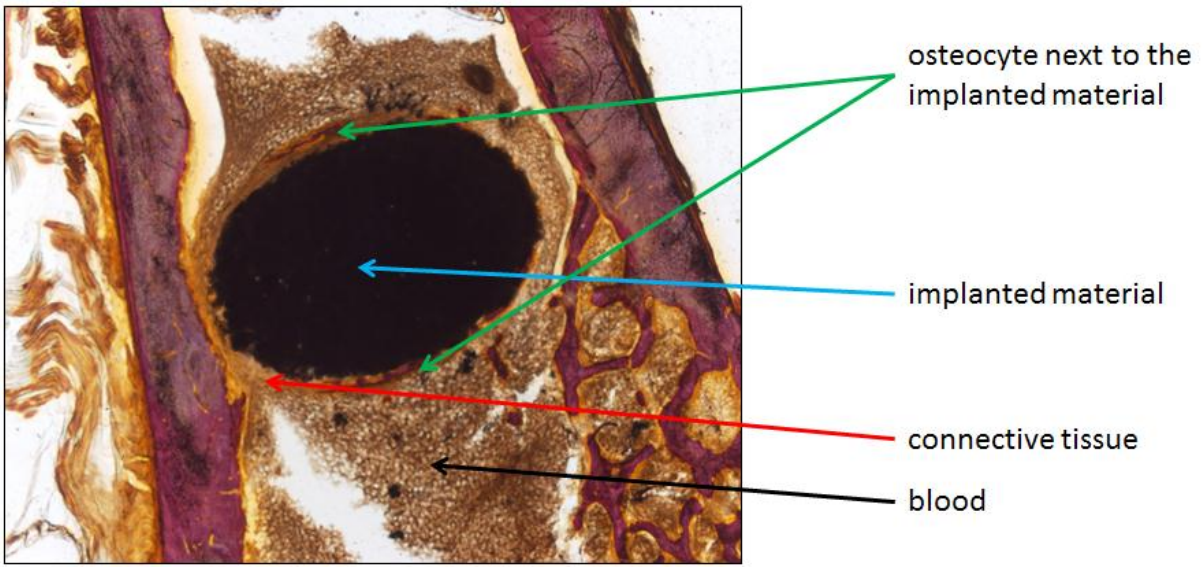

the implanted material (van Gieson, 5x):

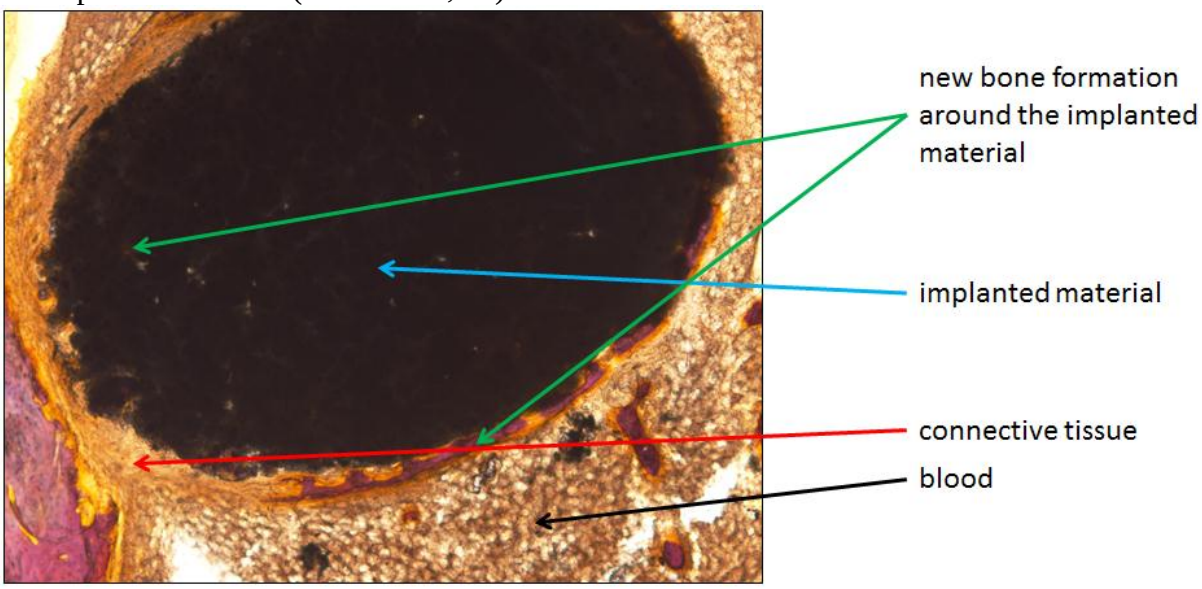

the implanted material in polarized light (van Gieson, 5x):

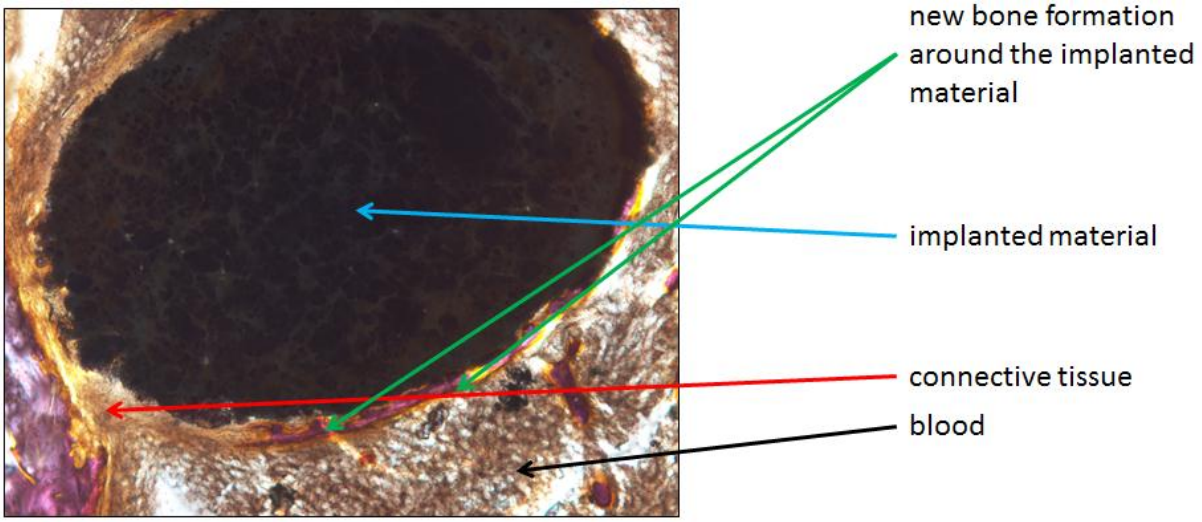

12 weeks after the surgical intervention
the implanted material (5x):

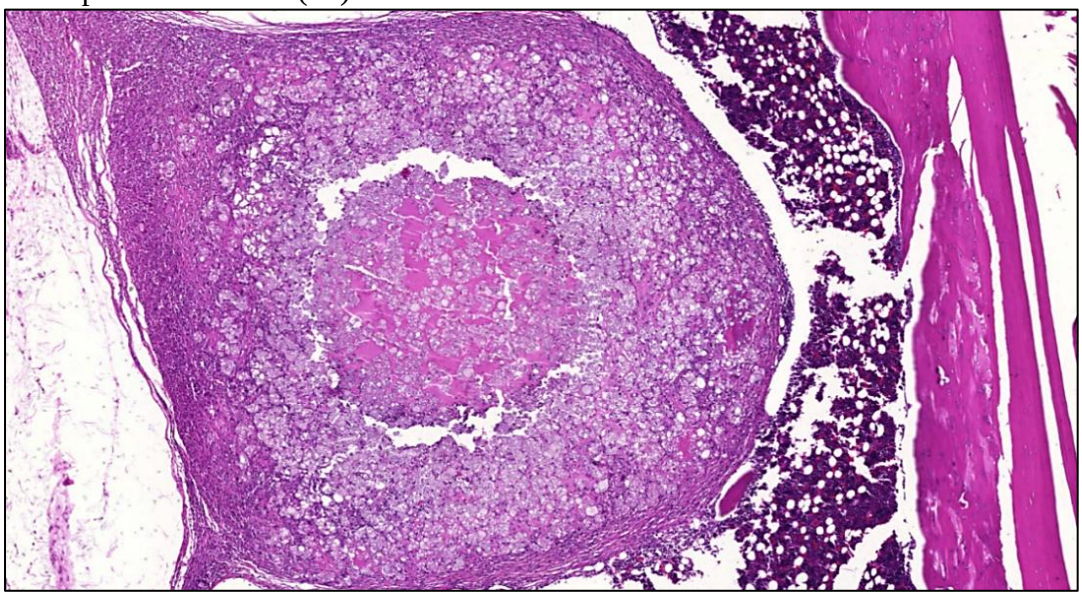

the implanted material (15x):

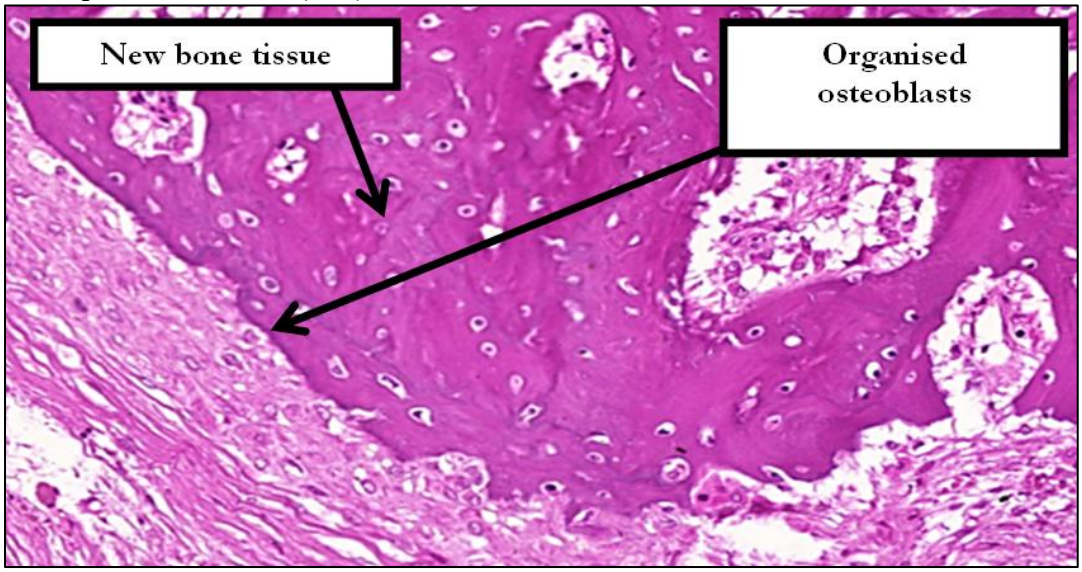

The following conclusion can be drawn from the histological examinations.

- In the control group only heamatoma and connective tissue formation could be seen near the drill hole, with no sign of bone formation.
- In the examined material next to connective tissue a few ostecytes can be seen even after 4 weeks.
- **After 8 weeks new bone formation could be seen around the implanted material and ostecytes began to appear inside the implanted material**.
- **After 12 weeks the number of new bone tissue appearance inside the implanted material was increased.**

Summarizing our results we can conclude that the bone substitution material developed inside the frame of the project proved to be a bioinert and osteoconductive material with adjustable pore size that is particularly suitable for further developing to human application.